The Astrophysical Journal Letters, 880:L5 (10pp), 2019 July 20 https://doi.org/10.3847/2041-8213/ab2a74


# Four Small Planets Buried in *K2* Systems: What Can We Learn for *TESS*?

Christina Hedges[1], Nicholas Saunders[1], Geert Barentsen[1], Jeffrey L. Coughlin[2], Josè Vinícius de Miranda Cardoso[3], Veselin B. Kostov[2,4], Jessie Dotson[5], and Ann Marie Cody[1]
[1] Bay Area Environmental Research Institute, P.O. Box 25, Moffett Field, CA 94035, USA; christina.l.hedges@nasa.gov
[2] SETI Institute, 189 Bernardo Avenue, Suite 200, Mountain View, CA 94043, USA
[3] Federal University of Campina Grande, Department of Electrical Engineering, Brazil
[4] NASA Goddard Space Flight Center, Greenbelt, MD 20771, USA
[5] NASA Ames Research Center, Moffett Field, CA 94035, USA
*Received 2019 April 23; revised 2019 May 24; accepted 2019 June 18; published 2019 July 18*

## Abstract

The *Kepler*, *K2*, and *Transiting Exoplanet Survey Satellite* (*TESS*) missions have provided a wealth of confirmed exoplanets, benefiting from a huge effort from the planet-hunting and follow-up community. With careful systematics mitigation, these missions provide precise photometric time series, which enable detection of transiting exoplanet signals. However, exoplanet hunting can be confounded by several factors, including instrumental noise, search biases, and host star variability. In this Letter, we discuss strategies to overcome these challenges using newly emerging techniques and tools. We demonstrate the power of new, fast open-source community tools (e.g., `lightkurve`, `starry`, `celerite`, `exoplanet`), and discuss four high signal-to-noise ratio (S/N) exoplanets that showcase specific challenges present in planet detection: *K2-43c*, *K2-168c*, *K2-198c*, and *K2-198d*. These planets have been undetected in several large *K2* planet searches, despite having transit signals with S/N $\geqslant$ 10. Two of the planets discussed here are new discoveries. In this work we confirm all four as true planets. Alongside these planet systems, we discuss three key challenges in finding small transiting exoplanets. The aim of this Letter is to help new researchers understand where planet detection efficiency gains can be made, and to encourage the continued use of *K2* archive data. The considerations presented in this Letter are equally applicable to *Kepler*, *K2*, and *TESS*, and the tools discussed here are available for the community to apply to improve exoplanet discovery and fitting.

*Key words:* methods: data analysis – planets and satellites: detection – surveys – techniques: photometric

## 1. Introduction

The *Kepler* mission (Borucki et al. 2010) has led to the detection of thousands of exoplanets, which have been used to further our understanding of planet occurrence rates and planet formation. After the loss of a second reaction wheel caused the *Kepler* spacecraft to lose fine pointing ability, the *Kepler* mission began a new phase, named *K2* (Howell et al. 2014). The *K2* mission has since lead to the detection of more than 350 confirmed, transiting planets, continuing the work from the *Kepler* mission.

The new *Transiting Exoplanet Survey Satellite* (*TESS*) mission (Ricker et al. 2014), launched in 2018, is building on the legacy of *Kepler* to provide an all-sky survey of nearby planet systems. In many ways, the data from *TESS* and *K2* are similar; both have short observing campaigns, are subject to sub-pixel spacecraft motion, and observe a significant number of young and active stars, in contrast to the original *Kepler* mission that focused on main-sequence FGK stars and benefited from extremely precise pointing stability. By better understanding our planet-hunting biases from *K2*, we can improve our efficiency in finding planets with both *K2* and *TESS*, and ultimately increase our planet detection efficiency.

In this work we undertake a planet search in existing planet systems from early *K2* campaigns, in order to demonstrate the power of new, open-source software to overcome key problems in planet-hunting searches with *K2* data. This simple search was not designed to be complete. Instead, it was designed to highlight cases where new tools offer significant benefits to the community, inspired by a recent study in which we concluded that hundreds more planets remain to be discovered in the *K2* data set (Dotson et al. 2019). This Letter aims to encourage the continued use of *K2* archive data by helping new and current researchers understand where improvements in transiting planet searches can continue to be made.

In this Letter we discuss three systems with confirmed transiting planets, where we have identified small planets that have remained unreported. These smaller planets have evaded detection for approximately 4 yr, despite several pipelines identifying the larger planets in the systems (Crossfield et al. 2016; Vanderburg et al. 2016; Mayo et al. 2018), and despite the unreported additional planets showing a high signal-to-noise ratio (S/N > 9). We present four additional planets in three systems in the following sections, and discuss in detail the factors we have identified that contributed to their being unreported. The S/N of small transiting planet signals can be improved by applying the analysis modifications presented in this Letter, increasing the likelihood of detection. If these simple methods are implemented in large pipeline searches for planets, they will increase planet detection efficiency, particularly for the *K2* and *TESS* missions.

The challenges discussed here are equally important for planets in *TESS* data. Likewise, the methods and tools that we have used to identify and fit these planets in *K2* data are equally applicable to *TESS* data. If unaddressed, these challenges may cause valuable multi-planet systems in *TESS* to also remain undetected.

In brief we discuss three key reasons that these particular planets have remained undiscovered.

1. High-frequency pointing jitter: the first three *K2* campaigns experienced increased levels of high-frequency

spacecraft motion. This intra-cadence noise is challenging to remove and can obscure small planet candidates by reducing the transit S/N.
2. Resonant planets: planets can naturally occur at orbital resonances, which cause peaks in the periodograms used to search for transiting signals to overlap with harmonics. Clipping out harmonics of significant peaks, or clipping transits, can reduce sensitivity to these resonant planets.
3. Stellar variability: high-amplitude stellar variability (e.g., from star spots) must usually be removed before searching for planets. If this variability is removed with an inadequate model, the residuals of the stellar variability model fit can be larger than any transiting planet signals, causing small planets to be lost in the noise.

In the following sections we present four planets, two of which are new discoveries, and two of which were previously identified as candidates in Pope et al. (2016), though unreported in the NASA Exoplanet Archive. In this work we confirm all four signals as true planet detections at greater than 95% confidence. In Section 2 we discuss the community tools and techniques that we have used to search and fit transiting planet signals. In Section 3 we first discuss our planet search and fitting methods. Each system is discussed in detail in Section 4, alongside a discussion of the factors that previously obscured these planets from being detected. We present full transit model fits for all planets in the systems (both previously identified, and discovered by this work) and vetting statistics for each planet. The scripts used to analyze each of the systems are available online.[6]

## 2. Background: Community Tools in *Kepler*, *K2*, and *TESS*

The *K2* mission provided the community with observations taken in ∼80 day campaigns, pointed toward the ecliptic plane. The roll motion of the spacecraft caused target motion relative to the detector of at most 2 pixels and typically $\lesssim$1 pixel. This roll motion generated characteristic noise in *K2* observations, caused by the point-spread function (PSF) of the star moving over sub-pixel sensitivity variations. Several attempts have been made to correct this noise, typically using one of three key methods: the self flat-fielding technique (SFF), pixel level decorrelation (PLD), and Gaussian process (GP) detrending. These methods have been used in several community pipelines: e.g., K2SFF (Vanderburg & Johnson 2014) and K2P2 (Lund et al. 2015) use SFF; EVEREST (Luger et al. 2016, 2018) uses PLD; and K2SC (Aigrain et al. 2016) and K2PHOT (Petigura et al. 2018) use GP detrending. These pipelines typically achieve a correction of the roll motion within a factor of 2–4 of the original *Kepler* precision.

Several new community tools have become available in the past year for working with *Kepler* data, producing light curves, removing instrument systematics and stellar variability, and discovering and fitting planet signals. These new tools and methods enable us to overcome the problems outlined in Section 1 and discussed in detail in Section 4, and find these planets that were previously buried in the noise. There are many new tools available to work with *Kepler*, *K2*, and *TESS* data.[7] The specific tools we have used in this Letter are listed below.

1. `lightkurve`[8] (Lightkurve Collaboration et al. 2018): a new open source Python package to work with *Kepler*, *K2*, and *TESS* data. Notably, `lightkurve` enables users to extract photometry using custom aperture masks, and remove motion systematics using tunable implementations of the SFF and PLD techniques.
2. `astropy.stats.BoxLeastSquares`[9] (Astropy Collaboration et al. 2013; Price-Whelan et al. 2018): a new, fast implementation of the box least squares (BLS; Kovács et al. 2002; Hartman & Bakos 2016) planet-finding algorithm in Python.
3. `exoplanet`[10] (Foreman-Mackey et al. 2019): a set of tools for fitting exoplanet transits and GPs to long-term trends using `pymc3`[11] based on the `starry`[12] and `celerite`[13] packages (Salvatier et al. 2016; Foreman-Mackey et al. 2017; Luger et al. 2019).

## 3. Method

### 3.1. Planet Search

In an effort to identify planets that have remained unreported in the NASA Exoplanet Archive we used the following approach. We selected only confirmed planet hosts from early campaigns 0 through 8, resulting in 164 stellar systems to search. These early campaigns have been archived at MAST for approximately 4 yr. We obtained the *Kepler* Pipeline (Jenkins et al. 2010) products from MAST, and used the Pre Data Search Conditioning Simple Aperture Photometry (PDCSAP) light curves of the existing planet host identified in the NASA Exoplanet Archive. We used a combination of GP detrending to remove long-term trends (for discussion of GPs and their application to time-series photometry, see Foreman-Mackey et al. 2017), and the SFF technique (see Vanderburg & Johnson 2014) to remove short-term *K2* roll motion systematics using `lightkurve`. We chose SFF for its simple implementation and speed. We generated hundreds of light curves for each target with varied motion detrending parameters and best-fit GP hyperparameters. We removed the signals of known planets by masking transits, and replaced them with Gaussian noise with the same standard deviation as the out-of-transit light curve. We then used `astropy.stats.BoxLeastSquares` to identify targets where there were signals of an additional transiting planet in a significant number of our hundreds of light curves.

Candidate transiting planets were identified by stacking BLS periodograms for each of the hundred light curves, and searching for over-densities that indicated a transiting signal in at least 10% of the detrended light curves, resulting in $\lesssim$10 candidate systems. These candidates were then inspected by eye, and systems with transit signals with S/N $\geqslant$ 4 were investigated in detail. We identified three systems with significant power in the BLS periodogram, which demonstrated common problems that are encountered in planet searches. We subsequently confirmed each of these planets (see Section 4). Once our candidates had been identified, we used a separate

[6] https://github.com/christinahedges/threemultis

[7] A full list of community tools for working with *Kepler*, *K2*, and *TESS* data can be found at https://docs.lightkurve.org/about/other_software.html.

[8] https://docs.lightkurve.org

[9] http://docs.astropy.org/en/latest/stats/bls.html

[10] https://exoplanet.dfm.io

[11] https://docs.pymc.io/

[12] https://rodluger.github.io/starry/

[13] https://celerite.readthedocs.io

method to produce more accurate light curves, as discussed in Section 3.2.

Our search of *K2* targets is by nature not complete, and is designed only to identify common pitfalls that have obscured planets from being identified in the *K2* data set. Our search is restricted only to confirmed planet systems from early campaigns. We vary only two of our detrending parameters; however, it would be possible to vary more parameters to improve completeness, including detrending method, pixel aperture size, and long-term detrending method. In this Letter we do not aim for completeness, and instead discuss three interesting case studies of planets that have been unreported, what factors have led to their obscurity, and how to alleviate these problems.

### 3.2. Planet Fitting

Once we had identified systems with significant evidence of additional planets, with a permissive threshold of $S/N \geqslant 4$, we recreated light curves using a slower but more accurate approach. We use `exoplanet` to simultaneously detrend spacecraft motion noise, using second-order PLD, and a GP to remove stellar variability using a Matérn $3/2$ kernel. We remove any transits from this step, to ensure that transits do not inform our estimate of the stellar variability. We then use our GP to predict the stellar variability during transits, and a Markov Chain Monte Carlo (MCMC) to estimate the uncertainties during transit, (which are slightly larger than the out-of-transit uncertainties). The uncertainties on each data point in the light curve have been marginalized over the uncertainties in our GP hyperparameters, meaning that they robustly capture our uncertainties from detrending. Preserving our uncertainties in our light curve allows us to accurately capture the uncertainties in our planet parameters.

Once we have our final light curve, we fit a multi-planet transit model using `exoplanet`, and use an MCMC to estimate the uncertainties on our planet parameters. The final results of our transit fit are given in Table 1, with $1\sigma$ uncertainties. For each transit fit we use literature values for stellar parameters from Dressing et al. (2017) and Mayo et al. (2018; see Table 1).

## 4. Results

### 4.1. K2-43

*K2-43* (EPIC 201205469) was observed in long cadence in Campaign 1 of the *K2* mission (program GO1059; PI: Stello), and Vanderburg et al. (2016) and Crossfield et al. (2016) discovered that it hosts a large, short-period planet. In early *K2* campaigns (C0-2), the spacecraft used a lower pointing control frequency that caused increased levels of intra-cadence motion compared to later *K2* campaigns (Van Cleve & Bryson 2017). This motion caused a significant change to the apparent measured PSF shape from frame to frame, as this motion was coadded during a single cadence. This apparent change in shape causes some motion detrending methods to fail. Methods such as SFF are fast and simple, and often provide excellent results. However, in the presence of intra-cadence motion, SFF can fail to produce the most accurate light curve, as the slight change in PSF shape causes changes to the target centroid, which is crucial to the success of the SFF method. The PLD method performs better on the extremely short-duration motion noise that is present in these early campaigns.

Early in the *K2* mission, systematics-corrected light curves were provided to the community by the K2SFF Pipeline (Vanderburg & Johnson 2014), which uses the SFF technique. Vanderburg et al. (2016), Dressing et al. (2017), and Mayo et al. (2018) used light curves from or using the same process as Vanderburg & Johnson (2014); Crossfield et al. (2016) built their own SFF light curves using a similar approach but modeling correlations between spacecraft roll and flux with a different method. As such, each of these works used methods that were unable to optimally correct the intra-cadence motion. *K2-43b* was identified in the SFF light curves, where the $S/N$ of the transits of a second planet *K2-43c* is low ($S/N < 9$). The small transiting planet signal was not identified, as it was buried in the high-frequency motion noise experienced by early *K2* campaigns. Using our method (described in Section 3.1) we identified weak evidence of a transiting planet *K2-43c*. After identifying the low $S/N$ signal, we built our refined light curve using the method discussed in Section 3.2, which greatly improved the $S/N$. By applying PLD detrending, the transit is identifiable as a $S/N > 10$ signal. Upon reviewing the EVEREST light curves, which also use PLD, and we find that *K2-43c* is also identifiable in the EVEREST community pipeline, which was released after K2SFF in 2016. Figure 1 shows the folded transits of *K2-43b* and the new planet identified in this work, *K2-43c*, using PLD detrending (see Section 3.2). Using PLD, the planet signal is robustly detected. Our best-fit planet model is shown in Figure 1 with $1\sigma$ uncertainties. The full planet parameters for our best-fit joint model of *K2-43b* and *c* are given in Table 1. We find *K2-43c* to have a radius of 2.42 $R_{\rm earth}$, and an orbital period of 2.42 days, resulting in an equilibrium temperature of 1000 K.

Using the planet-vetting tool `vespa` (see Morton 2012, 2015) we are able to assign a false positive probability (FPP) to both planets in the *K2-43* system. Similarly to many other works (including Crossfield et al. 2016 and Dressing et al. 2017), we adopt an FPP of $<1\%$ to validate a planet. We use direct-imaging contrast curves from the NIRC2 instrument at Keck II (obtained through ExoFOP) to rule out neighboring blended targets. Using the light curves that we have generated (see Figure 1), and stellar parameters derived by Dressing et al. (2017) for *K2-43*, we find an FPP of $<1e-6$ for *K2-43b*, and 0.00165 for *K2-43c*. Additionally, as discussed in Lissauer et al. (2012) and Sinukoff et al. (2016), we can apply a "multiplicity boost" to our probabilities, as systems with multiple planets are more likely to be true planets. Assuming the same multiplicity boost inferred for the *Kepler* mission (Lissauer et al. 2012), the FFP for *K2-43c* drops to $6.6104e-5$. Based on the small FPP, the absence of any known background stars, and a confirmed planet in the *K2-43* system, we label *K2-43c* as a confirmed planet. We also used the Discovery and Vetting of Exoplanets tool (DAVE) (Kostov et al. 2019) to ensure that there were no further signatures in the light curve that might indicate a false positive. We find no significant secondary eclipses for *K2-43c* and no significant odd–even differences between transits. As such, we confirm *K2-43c* as a true planet.

Dressing et al. (2017) highlighted that *K2-43b* is a good candidate for atmospheric observations with the *Hubble Space Telescope* and, in future, *James Webb Space Telescope* (*JWST*), due to the cool host star ($\sim$3800 K) that is relatively bright in

**Table 1**
Best-fit Parameters for all Known Planets in the *K2-43*, *K2-168*, and *K2-198* Systems

| | *K2-43 b* | *K2-43 c* |
|---|---|---|
| Period [days] | $3.471149\pm^{0.000104}_{0.000052}$ | $2.198884\pm^{0.000022}_{0.000011}$ |
| Transit Midpoint [JD] | $2456809.8843\pm^{0.00071}_{-0.00071}$ | $2456810.4059\pm^{0.0099}_{-0.0098}$ |
| Radius [$R_{\rm earth}$] | $4.51\pm^{0.44}_{0.19}$ | $2.42\pm^{0.26}_{0.11}$ |
| $R_P/R_*$ | $0.04298\pm^{0.002318}_{-0.001677}$ | $0.02319\pm^{0.001296}_{-0.001004}$ |
| Impact Parameter | $0.11\pm^{0.32}_{0.17}$ | $0.14\pm^{0.32}_{0.18}$ |
| Inclination [degrees] | $89.60\pm^{-1.35}_{-0.67}$ | $89.26\pm^{-1.85}_{-0.95}$ |
| Semi-major Axis [$a/R^*$] | $8.00\pm^{0.49}_{0.25}$ | $5.90\pm^{0.36}_{0.18}$ |
| Equilibrium Temperature [K] | $939.3\pm^{37.7}_{18.5}$ | $1093.7\pm^{43.9}_{21.5}$ |
| Stellar Mass [Msol] | $0.571\pm^{0.111}_{0.055}$ (Dressing et al. 2017) | |
| Stellar Radius [Rsol] | $0.542\pm^{0.049}_{0.022}$ (Dressing et al. 2017) | |
| Stellar Effective Temperature [K] | $3840.6\pm^{98.8}_{49.5}$ (Dressing et al. 2017) | |
| Limb Darkening 1 | $0.031\pm^{0.185}_{0.073}$ | |
| Limb Darkening 2 | $0.054\pm^{0.390}_{0.141}$ | |

| | *K2-168 b* | *K2-168 c* |
|---|---|---|
| Period [days] | $15.8523\pm^{0.0025}_{0.0012}$ | $8.050722\pm^{0.000075}_{0.000038}$ |
| Transit Midpoint [JD] | $2456975.03774\pm^{0.0023}_{-0.0023}$ | $2456973.7648\pm^{0.0100}_{-0.0099}$ |
| Radius [$R_{\rm earth}$] | $1.86\pm^{0.24}_{0.11}$ | $1.310\pm^{0.144}_{0.063}$ |
| $R_P/R_*$ | $0.01812\pm^{0.001}_{-0.0010}$ | $0.01258\pm^{0.00075}_{-0.00057}$ |
| Impact Parameter | $0.32\pm^{0.20}_{0.11}$ | $0.064\pm^{0.307}_{0.141}$ |
| Inclination [degrees] | $89.40\pm^{-0.46}_{-0.25}$ | $89.81\pm^{-0.98}_{-0.43}$ |
| Semi-major Axis [$a/R^*$] | $25.42\pm^{0.57}_{0.28}$ | $16.18\pm^{0.36}_{0.18}$ |
| Equilibrium Temperature [K] | $766.35\pm^{16.33}_{8.12}$ | $960.6\pm^{20.5}_{10.2}$ |
| Stellar Mass [Msol] | $0.877\pm^{0.060}_{0.029}$ (Mayo et al. 2018) | |
| Stellar Radius [Rsol] | $0.830\pm^{0.087}_{0.043}$ (Mayo et al. 2018) | |
| Stellar Effective Temperature [K] | $5502.7\pm^{101.0}_{50.5}$ (Mayo et al. 2018) | |
| Limb Darkening 1 | $0.10\pm^{0.40}_{0.19}$ | |
| Limb Darkening 2 | $0.083\pm^{0.501}_{0.206}$ | |

| | *K2-198 b* | *K2-198 c* | *K2-198 d* |
|---|---|---|---|
| Period [days] | $17.0428683\pm^{0.0000071}_{0.0000035}$ | $3.3596055\pm^{0.0000040}_{0.0000021}$ | $7.4500177\pm^{0.0000052}_{0.0000026}$ |
| Transit Midpoint [JD] | $2457204.5687\pm^{0.00014}_{-0.00014}$ | $2457215.0320\pm^{0.0019}_{-0.0017}$ | $2457213.5759\pm^{0.0010}_{-0.0010}$ |
| Radius [$R_{\rm earth}$] | $4.189\pm^{0.228}_{0.098}$ | $1.423\pm^{0.081}_{0.036}$ | $2.438\pm^{0.130}_{0.056}$ |
| $R_P/R_*$ | $0.039\pm^{0.0010}_{-0.00088}$ | $0.013\pm^{0.00037}_{-0.00032}$ | $0.022\pm^{0.00057}_{-0.00050}$ |
| Impact Parameter | $0.6610\pm^{0.0320}_{0.0099}$ | $0.715\pm^{0.030}_{0.012}$ | $0.047\pm^{0.226}_{0.104}$ |
| Inclination [degrees] | $88.904\pm^{-0.094}_{-0.027}$ | $86.494\pm^{-0.268}_{-0.088}$ | $89.86\pm^{-0.68}_{-0.30}$ |
| Semi-major Axis [$a/R^*$] | $25.86\pm^{0.95}_{0.48}$ | $8.76\pm^{0.32}_{0.16}$ | $14.90\pm^{0.55}_{0.28}$ |
| Equilibrium Temperature [K] | $715.80\pm^{18.72}_{9.26}$ | $1229.9\pm^{32.2}_{15.9}$ | $943.2\pm^{24.7}_{12.2}$ |
| Mass [Msol] | $0.799\pm^{0.091}_{0.045}$ (Mayo et al. 2018) | | |
| Radius [Rsol] | $0.757\pm^{0.035}_{0.016}$ (Mayo et al. 2018) | | |
| Effective Temperature [K] | $5212.9\pm^{99.0}_{49.2}$ (Mayo et al. 2018) | | |
| Limb Darkening 1 | $0.303\pm^{0.146}_{0.073}$ | | |
| Limb Darkening 2 | $0.25\pm^{0.23}_{0.11}$ | | |

**Note.** See Section 3.2 for details on the planet-fitting procedure. We find consistent parameters with literature results for previously confirmed planets *K2-43b, K2-168b,* and *K2-198b*.

the *K*-band ($K \sim 11.5$). *K2-43b* and *K2-43c* are on short periods, making observations more easily schedulable. The *K2-43* system could be an excellent candidate for comparative exoplanet atmosphere studies in a single system. However, as with many cool stars, the host star is a significantly spotted star, with flux variations of up to 5%, which may contaminate atmospheric transmission spectrum.

#### *4.1.1. What can We Learn for* TESS*?*

Similarly to *K2*, the *TESS* spacecraft is also subject to some amounts of motion due to spacecraft jitter (see the Tess Instrument Handbook; Vanderspek et al. 2018). Unlike the *K2* roll motion, this jitter causes targets to move randomly on the focal plane, with a magnitude of $\lesssim$1 pixel. In this case, the SFF detrending method will fail, as the motion on the detector is random, and a prediction for the flux at a given pixel

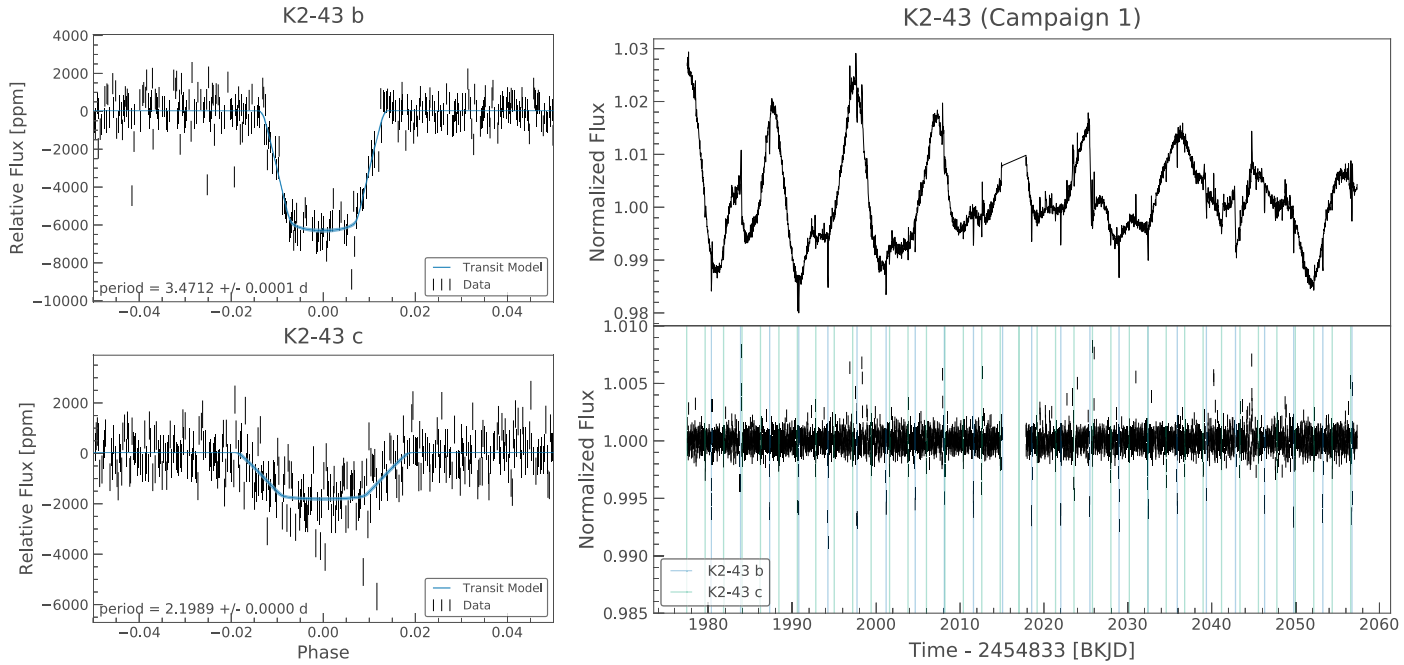


**Figure 1.** Left panels: folded transits of *K2-43b* and *c*, having simultaneously removed *K2* motion systematics and long-term stellar variability (see Section 3.2. Our best-fit planet model is show in blue alongside the $1\sigma$ uncertainty. Right panels: light curves of *K2-43*. Top row: light curve with motion systematics corrected. Strong stellar variability due to spots is clearly evident. Bottom row: light curve with both motion systematics and stellar variability removed. Transits of *K2-43b* and *c* have been highlighted.

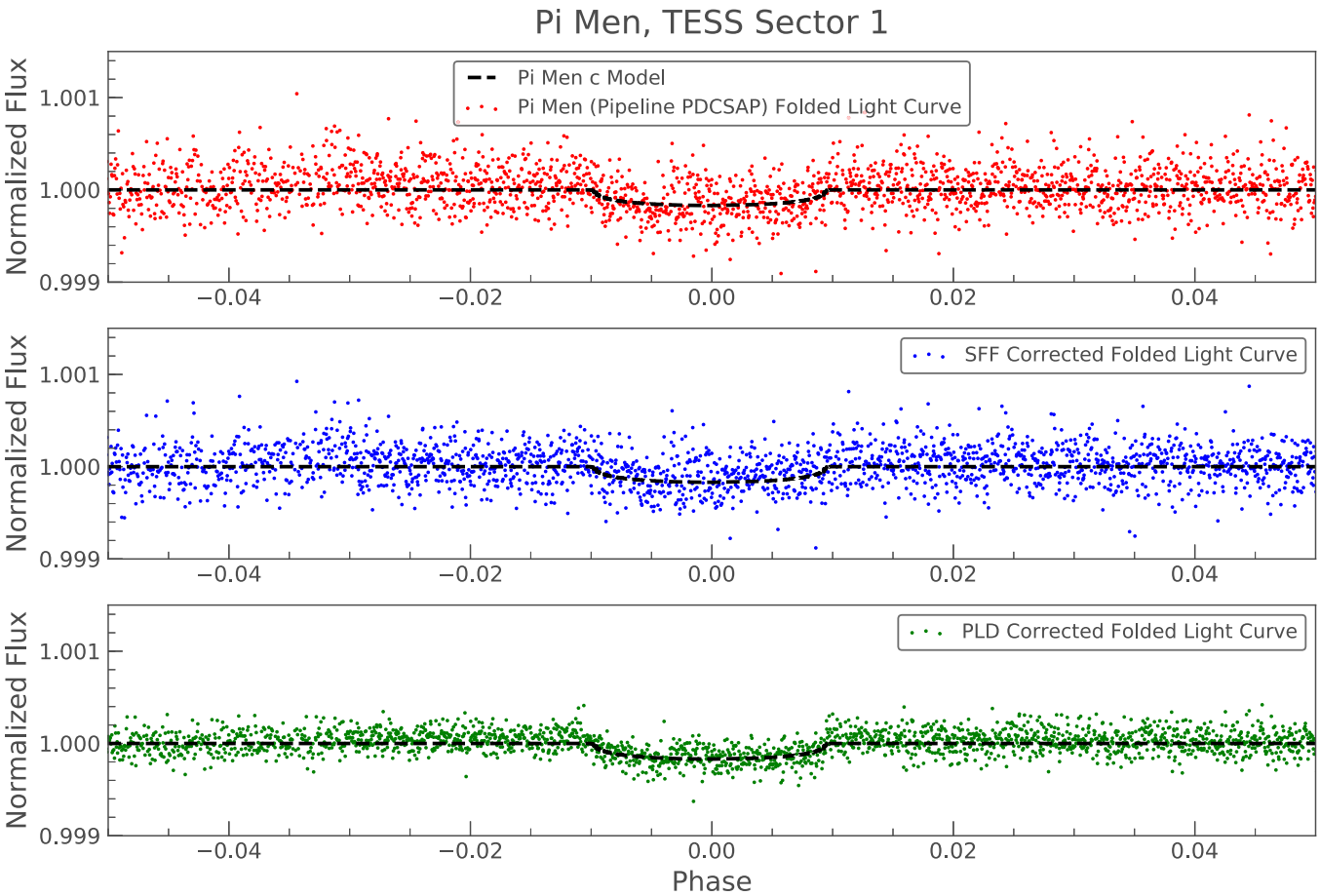


**Figure 2.** Example of TESS light curve for planet pi Men c from Sector 1. Top panel: pre-searched data conditioning light curve from the NASA pipeline. Middle row: PDCSAP light curve, corrected using SFF. Bottom panel: PDCSAP light curve, corrected using PLD. The PDCSAP and SFF light curves have a comparable scatter, with a combined differential photometric precision (CDPP; see Jenkins et al. 2010) of 54 and 58, respectively. The PLD method has better removed the *TESS* spacecraft jitter, and achieves a CDPP of 32.

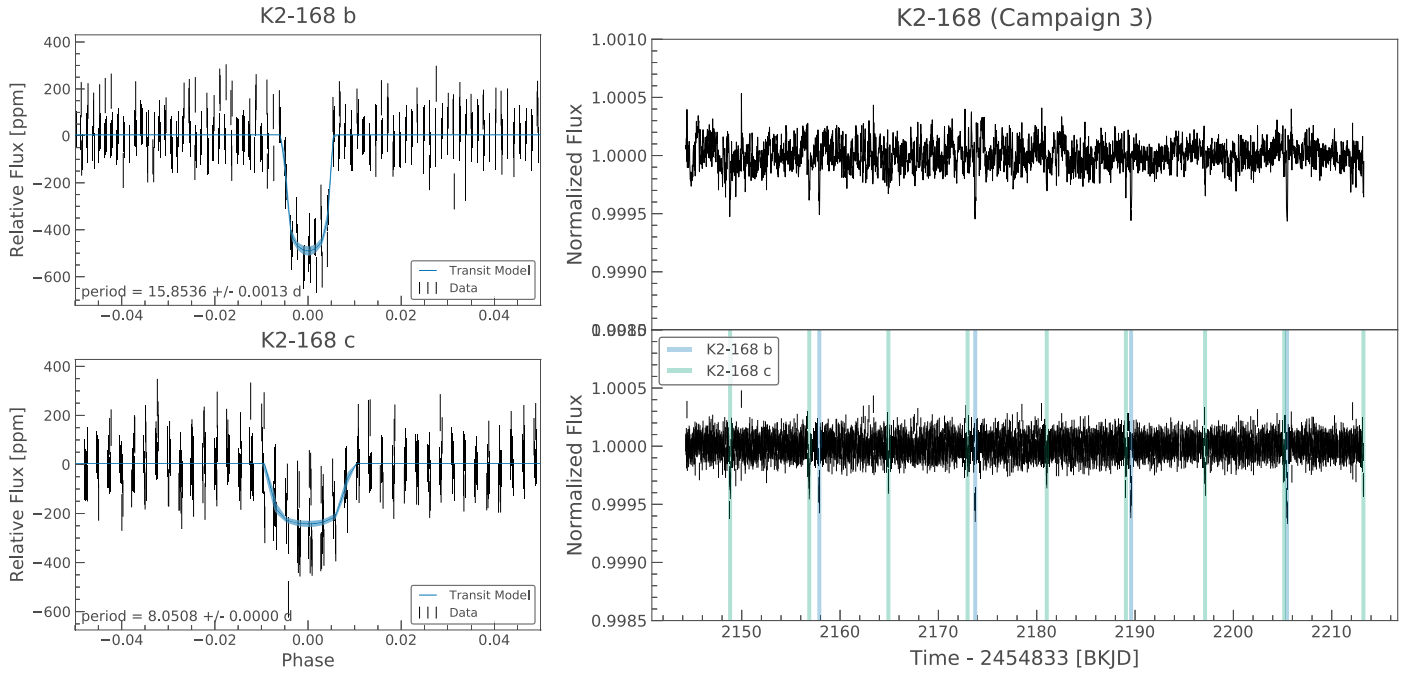


**Figure 3.** Left panels: folded transits of *K2-168b* and *c*, having simultaneously removed *K2* motion systematics and long term stellar variability (see Section 3.2). Our best-fit planet model is show in blue with the $1\sigma$ uncertainties. Right panels: light curves of *K2-168*. Top row: light curve with motion systematics corrected. Bottom row: light curve with both motion systematics and stellar variability removed. Transits of *K2-168b* and *c* have been highlighted. Most of the transits of *K2-168b* occur close to transit of *K2-168c*.

location cannot be estimated. The PLD method is not dependent on estimating the centroid position of the PSF, or fitting an arclength to its motion. Instead, PLD relies solely on the correlation between changing flux intensity measured by pixels on the detector. This allows PLD to extract correlated noise signals caused by random motion with sub-pixel magnitude, and has been shown to effectively remove jitter noise from *Spitzer* observations (Deming et al. 2015). In order to improve light curve quality for planet hunting with *TESS*, we recommend using PLD to detrend spacecraft jitter.

Figure 2 shows an example of a *TESS* light curve when *TESS* jitter is removed. We use confirmed *TESS* planet pi Men c as an example. The NASA pipeline Pre-search Data Conditioning light curve, an SFF correction, and a PLD correction are shown. The reduction in noise for *TESS* is >50% if PLD is used, compared to using either the NASA pipeline-provided light curve or an SFF detrending. This shows the benefit of removing *TESS* jitter, in particular by employing the PLD method.

Open-source implementations of systematic removal methods are now readily available. The `lightkurve` package provides an open-source, Python interface for working with *Kepler*, *K2*, and *TESS* data. This includes data access from the MAST archive, the generation of light curves from the calibrated image data, and removal of common instrument systematics. `lightkurve` provides a way for users to implement simple versions of both SFF and PLD on any of these data sets, and remove systematics such as the *K2* roll motion and *TESS* jitter. `lightkurve` is also tunable, allowing users to iterate over detrending parameters to establish the effect of the detrending on their final light curve.

### 4.2. K2-168

*K2-168* (EPIC 205950854) was observed in long cadence in the *K2* campaign 3 (program PIs: Petigura, GO3104; Sanchis-Ojeda, GO3054), and was identified by Vanderburg et al. (2016) and Mayo et al. (2018) as hosting a super-Earth-sized planet on a 15.8 day orbit. We have identified a second planet in the system, in a near orbital resonance, with an 8.1 day period.[14] Figure 3 shows our best fit of both planets. The full planet parameters for our best fit joint model of *K2-168b c* are shown given in Table 1. The transit signal of this new planet is detectable in all three of the publicly available community light curve databases that are hosted at MAST (K2SFF, EVEREST, and K2SC). However, the transit of *K2-168c* can have low signal to noise in some planet discovery pipelines because of its near resonance with *K2-168b*.

The period of *K2-168c* is almost exactly half the period of *K2-168b*, ($P_b/P_c = 1.969$), causing the BLS peak for *K2-168c* to occur close to a harmonic peak from *K2-168b*. If, when searching for multiple transiting planets, these resonant peaks were removed, this planet would go undetected. Furthermore, the transits of *K2-168c* also occur close to transits of *K2-168b* in time. If transits of *K2-168b* were removed before searching for multiple transiting planets, many of the transits of *K2-168c* would also be removed. This rare situation, where a second resonant planet is also close in phase, would be alleviated in a mission with a longer baseline, where the planets would eventually drift apart. However, for a short baseline mission

[14] After submission of this Letter, Heller et al. (2019) identified this signal as a transiting planet candidate using the `tls` algorithm Hippke & Heller (2019). The TLS algorithm fits a true transit shape rather than the BLS box, which is similar to the original pipeline process, and can increase the signal to noise of small planet candidates (for a discussion, see the *Kepler* Data Processing Handbook; Li et al. 2017).

such as *K2*, it is possible to have most of the transits overlap, causing shallow transits of resonant planets to remain undetected.

In some planet-hunting pipelines (including Vanderburg et al. 2016; Mayo et al. 2018; and the original *Kepler* pipeline Jenkins et al. 2010), transits are clipped with a small margin before performing a second transit search, in order to identify multi-planet systems. For example, both Vanderburg et al. (2016) and the original *Kepler* pipeline remove points within 1.5 days of the transit midpoint. This practice can reduce the signal to noise of planets such as *K2-168c*, where transit clipping K2-168b would remove the number of observed transits from 9 to 6. Following the method in Vanderburg et al. (2016), the S/N of the K2-168 c transit is 5.8 if transits are clipped, and 7.2 if transits are not clipped. Vanderburg et al. (2016) and Mayo et al. (2018) required an S/N of 9 before a signal is considered a planet candidate, and so this small signal would not have been detected in either pipeline, even if transits were not clipped. However, this modest increase in S/N and number of transits observed can easily be the difference between a planet signal being triggered in a pipeline and it remaining undetected.

Using the same method as for *K2-43*, we have calculated the FPP for *K2-168b* and *c*. No contrast curves are available for *K2-168*, and so our FPP values are slightly higher. Using the light curves that we have generated (see Figure 3), and the stellar parameters derived by Mayo et al. (2018) for *K2-168*, we find an FPP of $4.719e{-}5$ for *K2-168b*, and 0.0204 for *K2-168c* using `vespa`. While the FPP for *K2-168c* is slightly larger than 1%, when we apply the multiplicity boost from Lissauer et al. (2012) we find a FPP of 0.00083 for *K2-168c*. Owing to the multiplicity boost, we can label *K2-168c* as a confirmed planet. We also ran vetting tools from the DAVE pipeline and find no significant secondaries or odd–even transit depth differences for *K2-168*. We also find no significant centroid shifts, which would indicate the signal originates from a background star.

Resonant multi-planet systems are particularly valuable for exoplanet science. These systems are likely to exhibit measurable transit timing variations (TTVs), which enable the derivation of mass estimates for planets. *K2-168* is a system close to a 2:1 resonance, suggesting that it may exhibit TTVs, though we do not detect significant evidence of TTVs during the short ∼80 day *K2* observation. Additionally, both planets are close to the radius gap observed in *Kepler*, where literature has noted a deficit of planets with $R \sim 1.5$–$2\ R_{\rm earth}$ (Fulton et al. 2017). *K2-168* may provide an interesting insight into planet formation close to this boundary. It is important that resonant systems are identified, particularly in missions such as *K2* and *TESS*, where planet formation around a variety of stellar types can be understood.

#### 4.2.1. What can We Learn for TESS?

Like *K2*, the *TESS* mission has a short baseline of observation for the majority of targets. While those targets in the continuous viewing zone will have a baseline of up to 1 yr, most targets in the *TESS* prime mission have continuous observations for only 27 days. Systems similar to *K2-168*, where transits from resonant small planets are buried in the harmonics of larger planets, will be difficult to separate in *TESS*. Extra care should be taken to identify these valuable systems. 75% of *TESS* targets will be observed for only a single 27 day sector, and 95% of *TESS* targets will be observed for three sectors or less (see Barclay et al. 2018). As such, the majority of *TESS* targets will have a short baseline, and resonant multi-planet *TESS* systems will be susceptible to this problem.

The new `exoplanet` Python package enables users to simultaneously fit multiple planet systems, benefiting from the fast, stable, and differentiable analytical transit models provided by the `starry` package. `exoplanet` is able to simultaneously fit transits, long-term instrument systematics, and long-term stellar variability using Gaussian processes. The loss of additional resonant planets can be avoided by employing `exoplanet` to robustly fit and remove exoplanet transits before searching for signatures of additional planets, rather than removing harmonics from the BLS power spectrum or removing transits from the light curve.

### 4.3. K2-198

*K2-198* (EPIC 212768333) was observed in long cadence in *K2* campaign 6 (program PIs: Jackson, GO6029; Howard, GO6030; Stello, GO6032; Charbonneau, GO6069; Thompson, GO6086; Dragomir, GO6087). Mayo et al. (2018) identified a large $\sim 4\ R_{\rm earth}$ exoplanet. The system was also observed later, in campaign 17. *K2-198* exhibits significant stellar variability, likely from star spots (see Figure 4). This spot modulation is approximately 3% in amplitude, which is much larger than the signal of the transits. If this modulation is not adequately removed, it will suppress signals from a transiting planet.

A common approach to removing stellar variability is to use some form of smoothing filter (e.g., a median or Savitzky-Golay filter). For example, Mayo et al. (2018) and Vanderburg et al. (2016) used a basis spline to remove long-term trends. These approaches are fast and simple, making it ideal for planet searches where thousands of light curves must be whitened to remove stellar variability before a planet-finding algorithm (e.g., BLS) can be applied. However, such smoothing kernels have two key drawbacks. First, these kernels smooth over any existing planet transits that have not been masked, reducing their transit depth. Second, in cases where planet transits are masked, these kernels cannot be used to predict the stellar variability during masked times. As such, there is no way to mask transits and accurately preserve their transit depths. Using GPs to accurately model stellar variability overcomes these two issues (see Foreman-Mackey et al. 2017 for a discussion of the application of GPs in the time domain). GPs are able to robustly predict the stellar variability during masked cadences. Furthermore, it is possible to marginalize over the uncertainties in the best-fit GP model hyperparameters, enabling users to accurately estimate the uncertainties due to model uncertainty during transits. As such, a GP is a more reliable method for removing stellar variability, prior to searching for transits. While overcoming stellar variability is a common problem, attempted by all planet-hunting pipelines, the use of GPs to remove this variability is quite new, and new tools are now available to the community to easily implement this technique (e.g., `celerite`).

In the case of *K2-198*, we have identified two small planets at shorter periods than *K2-198b* that are only detectable when the long-term stellar variability is removed using a GP. Planets *c* and *d* were not identified in Mayo et al. (2018), who employed a basis spline correction at 1.5 days to remove long-term trends. While not reported on the NASA Exoplanet Archive, Pope et al. (2016) identified both *c* and *d* as candidate

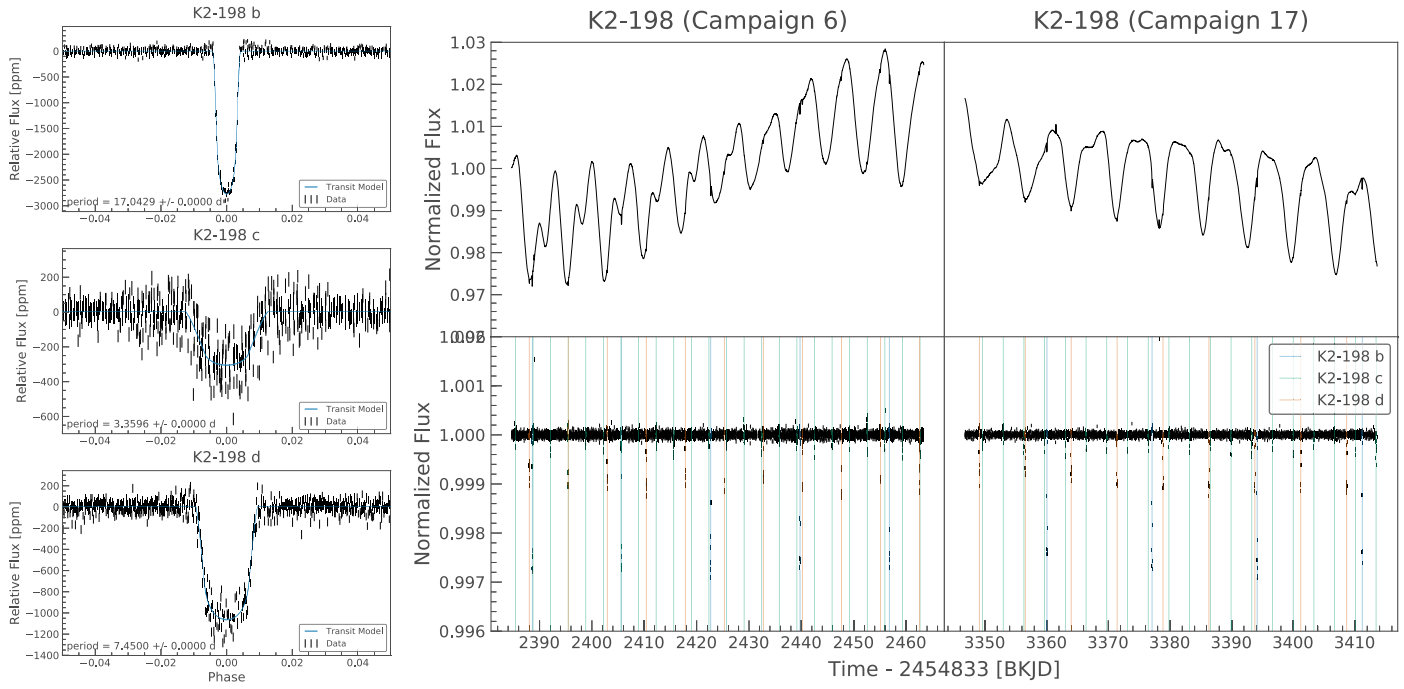


**Figure 4.** Left panels: folded transits of *K2-198b, c*, and *d*, having simultaneously removed *K2* motion systematics and long-term stellar variability (see Section 3.2). Our best-fit planet model is show in blue alongside the $1\sigma$ uncertainty. Right panels: light curves of *K2-198*. Top row: light curve with motion systematics corrected. Strong stellar variability due to spots is clearly evident. Bottom row: light curve with both motion systematics and stellar variability removed. Transits of *K2-198b, c*, and *d* have been highlighted.

transits, by employing GP detrending to remove stellar variability.

Figure 4 shows the folded transits of all planets in the *K2-198* system, and the removed best-fit stellar variability model, using a GP with a Matérn 3/2 kernel. We fit our long-term stellar trend simultaneously with our motion systematics removal (see Section 3.2) and robustly propagate the uncertainties by marginalizing over our GP hyperparameters. Figure 4 clearly shows that the transits are detectable only after the stellar variability is accurately removed. The full planet parameters for our best-fit joint model of *K2-198b*, *c*, and *d* are shown given in Table 1. *K2-198* was observed in both K2 campaign 6 and campaign 17. After we identified these three transits in the campaign 6 data, we added the campaign 17 data in our improved light curve (see Section 3.2) in order to obtain the best planet parameter fits. We find that *c* and *d* have radii of 1.4 and 2.4 $R_{\rm earth}$, respectively, with orbital periods of 3.35 and 7.45 days.

Using the same method as for *K2-43* above, we have calculated the FPP for the *K2-198* system. We use contrast curves from direct imaging to rule out close background stars, and inform our FPP prediction. Contrast curves for *K2-198* from the Palomar High Angular Resolution Observer (PHARO) instrument at the Palomar telescope (Hayward et al. 2001) and the Differential Speckle Survey Instrument (DSSI) at the WIYN telescope (Howell et al. 2011) are available on ExoFOP. Using the light curves that we have generated (see Figure 4), and stellar parameters derived by Mayo et al. (2018) for *K2-198*, we find an FPP of $< 1e{-}6$ for *K2-198b*, 0.000425 for *K2-198c*, and $<1e{-}6$ for *K2-198d* using `vespa`. Without employing any multiplicity boost, we are able to label *K*2-198*c* and *d* confirmed planets. We used the DAVE pipeline to find that there are no significant secondaries or odd–even transit depth differences for *K2-198d*. While the pipeline failed to process *K2-198c*, we consider it to be a confirmed planet based on its low FPP.

*K2-198* is at least a three-planet system. Multiple systems with large numbers of planets are particularly useful to test planet formation models and understand the dynamics of planetary systems. Additionally, similarly to *K2-168c*, *K2-198c* is close to the exoplanet radius boundary, increasing the system's potential to test planet formation models, making *K2-198* a valuable system.

#### 4.3.1. What can We Learn for TESS?

Stellar variability is likely to be a confounding factor for many important *TESS* planet discoveries. In particular, valuable planet discoveries around young stars are likely to be obscured by large star spots (e.g., see the recent *K2* discovery of a planet around a variable young star; David et al. 2019). Planets around small cool stars (which are excellent targets for atmospheric characterization with *JWST*), are also likely to have large stellar variability. Removing this stellar variability accurately is crucial to planet searches around these stars. The original *Kepler* mission targeted primarily solar-like stars, which are naturally less variable, and vary on longer timescales, making stellar variability less problematic than for the *K2* and *TESS* missions. The *K2* and *TESS* catalogs contain many more young and active stars, where GPs can be highly beneficial for removing stellar variability.

There are several open source packages to mitigate stellar variability that are relevant for *Kepler*, *K2*, and *TESS*. In particular, the `celerite` package provides a fast implementation of a GP for 1D time-series data. `celerite` can be used as an alternative to simple smoothing filters to remove long-term stellar variability and improve light curves for exoplanet hunting. Additionally, the `exoplanet` package provides utilities to fit GP models simultaneously with transit models,

allowing the uncertainties associated with fitting the stellar variability to be propagated into the planet parameters.

## 5. Conclusions

In this Letter we discuss and confirm four *K2* planets and provide vetting statistics to confirm them. Each planet was found in a *K2* system that was already known to host a confirmed planet. We have used `vespa` to confirm these planets and find low FPPs for each planet. Analysis with DAVE shows that there are no significant secondary or tertiary eclipses, odd–even differences between consecutive transits, or photocenter shifts during transits for *K2-43 c*, *K2-168 c*,and *K2-198 d*, confirming the planetary interpretation of the transits. Our discoveries suggest that there are still many planets waiting to be found in the *K2* data set. Two of the planets that we have presented here are close to the planet radius gap (Fulton et al. 2017), thus increasing the value of the *K2* planet sample to study this gap.

In this work we have performed a search for low S/N transiting planet signals in known *K2* planet systems. From this search, we identified four candidates that were not reported in the NASA Exoplanet Archive, and showcased key problems that have confounded exoplanet searches in *K2*. In this work we have confirmed each planet, discussed the confounding factors in detail, and signposted new open-source tools that can be used to overcome each problem. Our search was not designed to be complete, and was instead designed to highlight new methods that can be easily implemented to find new planets in the *K2* data set, and by extension the *TESS* data set.

We find that the following factors confounded transit searches for the three systems presented here. (1) Instrument motion systematics (such as the *K2* roll motion), particularly those on short timescales of $\lesssim$1 cadence, can cause noise that buries planet signals. These systematics can be carefully removed in conjunction with stellar systematics in order to reach the highest possible precision (see Sections 4.1 and 3.2). (2) Multi-planet systems where planets naturally occur close to resonances can be difficult to identify, particularly if the baseline of the observation is comparable to the orbital period of the planets (see Section 4.2). (3) The long-term stellar variability of the host star can obscure the planet transit signals, if not removed using an appropriate method (see Section 4.3). Each of these key factors that have affected the *K2* systems presented here are equally important for the recently commissioned *TESS* mission.

The data used to find these planets has been analyzed by several teams, and processed by several planet-hunting pipelines. However, these signals have evaded detection by major pipelines. It has also been shown by previous work using the *Kepler* detection efficiency that there are more planets to be found in the *K2* data set (e.g., Dotson et al. 2019), and that multi-planet systems have been under-reported in the *Kepler* data set (see Zink et al. 2019). The discovery of these planets in known systems highlights that there may indeed be many more planets waiting to be found in the *K2* data, if the challenges discussed in this work are addressed. While *Kepler* focused primarily on quiet stars, where stellar variability is a lower magnitude effect, gains could potentially still be made by robustly removing stellar variability with a GP before planet searching in the *Kepler* data set.

These challenges can be addressed using new open-source community tools. Two common motion systematics mitigation techniques (SFF and PLD) are now available in the new `lightkurve` toolkit. The new fast implementation of BLS, now in available in `astropy.stats.BoxLeastSquares`, can be used in conjunction with `lightkurve` to iteratively search for planets while varying systematics removal parameters, and masking known transits. The new `exoplanet` package, based on the `starry` and `celerite`, can implement fast exoplanet transit modeling and the removal of stellar variability using GPs. These toolkits are ready to be applied to both *K2* and *TESS* archival data to find empower a comprehensive survey of high-value small planets in multi-planet systems, further expanding the legacy of NASA's exoplanet finding missions.

This Letter uses several community tools, and we would like to thank all of the authors of these community packages for documenting and releasing their code. In particular, we would like to recognize the exceptional efforts by Daniel Foreman-Mackey, Rodrigo Luger, and Timothy Morton. This Letter includes data collected by the *K2* mission and obtained from the MAST data archive at the Space Telescope Science Institute (STScI). Funding for the *K2* mission is provided by the NASA Science Mission Directorate. STScI is operated by the Association of Universities for Research in Astronomy, Inc., under NASA contract NAS 526555. This research has made use of the NASA Exoplanet Archive, which is operated by the California Institute of Technology, under contract with the National Aeronautics and Space Administration under the Exoplanet Exploration Program. This Letter has made use of the ExoFOP service, which is funded by NASA through the NASA Exoplanet Science Institute.

*Facilities: Kepler*, MAST, Exoplanet Archive.

## ORCID iDs

Christina Hedges https://orcid.org/0000-0002-3385-8391
Geert Barentsen https://orcid.org/0000-0002-3306-3484
Jeffrey L. Coughlin https://orcid.org/0000-0003-1634-9672
Veselin B. Kostov https://orcid.org/0000-0001-9786-1031
Jessie Dotson https://orcid.org/0000-0003-4206-5649
Ann Marie Cody https://orcid.org/0000-0002-3656-6706

## References

Aigrain, S., Parviainen, H., & Pope, B. J. S. 2016, MNRAS, 459, 2408
Astropy Collaboration, Robitaille, T. P., Tollerud, E. J., et al. 2013, A&A, 558, A33
Barclay, T., Pepper, J., & Quintana, E. V. 2018, ApJS, 239, 2
Borucki, W. J., Koch, D., Basri, G., et al. 2010, Sci, 327, 977
Crossfield, I. J. M., Ciardi, D. R., Petigura, E. A., et al. 2016, ApJS, 226, 7
David, T. J., Cody, A. M., Hedges, C. L., et al. 2019, arXiv:1902.09670
Deming, D., Knutson, H., Kammer, J., et al. 2015, ApJ, 805, 132
Dotson, J. L., Barentsen, G., Hedges, C., & Coughlin, J. L. 2019, RNAAS, 3, 23
Dressing, C. D., Vanderburg, A., Schlieder, J. E., et al. 2017, AJ, 154, 207
Foreman-Mackey, D., Agol, E., Angus, R., & Ambikasaran, S. 2017, AJ, 154, 220
Foreman-Mackey, D., Barentsen, G., & Barclay, T. 2019, dfm/exoplanet: exoplanet, v0.1.4, Zenodo, doi:10.5281/zenodo.2561395
Fulton, B. J., Petigura, E. A., Howard, A. W., et al. 2017, AJ, 154, 109
Hartman, J. D., & Bakos, G. Á. 2016, A&C, 17, 1
Hayward, T. L., Brandl, B., Pirger, B., et al. 2001, PASP, 113, 105
Heller, R., Hippke, M., & Rodenbeck, K. 2019, A&A, 627, A66
Hippke, M., & Heller, R. 2019, A&A, 623, A39

Howell, S. B., Everett, M. E., Sherry, W., Horch, E., & Ciardi, D. R. 2011, AJ, 142, 19
Howell, S. B., Sobeck, C., Haas, M., et al. 2014, PASP, 126, 398
Jenkins, J. M., Caldwell, D. A., Chandrasekaran, H., et al. 2010, ApJL, 713, L87
Kostov, V. B., Mullally, S. E., Quintana, E. V., et al. 2019, AJ, 157, 124
Kovács, G., Zucker, S., & Mazeh, T. 2002, A&A, 391, 369
Li, J., Tenenbaum, P., & Twicken, J. D. 2017, Kepler Data Processing Handbook: Data Validation II. Transit Model Fitting and Multiple Planet Search, Kepler Science Document KSCI-19081-002
Lightkurve Collaboration, Cardoso, J. V. D. M., Hedges, C., et al. 2018, Lightkurve: Kepler and TESS Time Series Analysis in Python, Astrophysics Source Code Library, ascl:1812.013
Lissauer, J. J., Marcy, G. W., Rowe, J. F., et al. 2012, ApJ, 750, 112
Luger, R., Agol, E., Foreman-Mackey, D., et al. 2019, AJ, 157, 64
Luger, R., Agol, E., Kruse, E., et al. 2016, AJ, 152, 100
Luger, R., Kruse, E., Foreman-Mackey, D., Agol, E., & Saunders, N. 2018, AJ, 156, 99
Lund, M. N., Handberg, R., Davies, G. R., Chaplin, W. J., & Jones, C. D. 2015, ApJ, 806, 30
Mayo, A. W., Vanderburg, A., Latham, D. W., et al. 2018, AJ, 155, 136
Morton, T. D. 2012, ApJ, 761, 6
Morton, T. D. 2015, VESPA: False Positive Probabilities Calculator, Astrophysics Source Code Library, ascl:1503.011
Petigura, E. A., Crossfield, I. J. M., Isaacson, H., et al. 2018, AJ, 155, 21
Pope, B. J. S., Parviainen, H., & Aigrain, S. 2016, MNRAS, 461, 3399
Price-Whelan, A. M., Sipőcz, B. M., Günther, H. M., et al. 2018, AJ, 156, 123
Ricker, G. R., Winn, J. N., Vanderspek, R., et al. 2014, Proc. SPIE, 9143, 914320
Salvatier, J., Wiecki, T. V., & Fonnesbeck, C. 2016, PeerJ Computer Science, 2, e55
Sinukoff, E., Howard, A. W., Petigura, E. A., et al. 2016, ApJ, 827, 78
Van Cleve, J. E., & Bryson, S. T. 2017, K2 Handbook, Kepler Science Document KSCI-19116-001
Vanderburg, A., & Johnson, J. A. 2014, PASP, 126, 948
Vanderburg, A., Latham, D. W., Buchhave, L. A., et al. 2016, ApJS, 222, 14
Vanderspek, R., Doty, J. P., & Fausnaugh, M. 2018, TESS Instrument Handbook, STScI, https://archive.stsci.edu/missions/tess/doc/TESS_Instrument_Handbook_v0.1.pdf
Zink, J. K., Christiansen, J. L., & Hansen, B. M. S. 2019, MNRAS, 483, 4479